INVESTIGATING EQUAL X-RAY BODIES TO THE TRIANGLE

DAVID MILLER

ADVISOR: DR. D.C. SOLMON
OREGON STATE UNIVERSITY

ABSTRACT. In this paper we will examine the directed X-Rays generated by two sources in order to determine whether there exists any convex body sharing the same X-Rays as a triangle.

1. INTRODUCTION

The field of geometric tomography concerns what properties of figures may be determined from generalized x-rays passing through the figures. The question that birthed the field was posed by Hammer [6] in 1961. Since that time, some situations have been thoroughly analyzed. Falconer [2] and Gardner [5] proved in 1983 that x-rays from two sources, positioned such that the line through the sources passes through the figure, were enough to determine a convex figure entirely. Building on this work, Volcic [8] showed, in 1986, that a convex figure could be determined by three non-collinear x-ray sources. It is currently unknown if two x-ray sources, whose connecting line does not pass through the figure, are enough to determine a convex shape.

Fithian [3] investigated this situation with specific interest in determining the x-ray uniqueness of triangles. Utilizing several theorems discussed within [3], he was able to show that in all but a single configuration of triangle vertices, no equal x-ray body could exist. This last case is illustrated below in Figure 3. Fithian continued work on this last case in a later paper [4], but was unable to show that no secondary body existed. All evidence he had discovered up until then has pointed to the secondary body not existing.

This paper began as a continuation of Fithian's work into this remaining case. Results in the first section of the paper were derived in order to attempt to prove the hypothesis that the equal x-ray body did not exist. Newer numerical calculation, carried out via the computer program *Geometer's Sketchpad* pointed to the possibility of the secondary body existing, and thus later results were derived with the goal of finding such a body.

Results are divided into three main sections:

(1) Derivative Results
(2) Distance Results
(3) Existence Results

2. NOTATION AND DEFINITIONS

All work takes place in the plane $\mathbb{R}^2$.

Date: 8/14/05.
This work was done during the Summer 2005 REU program in Mathematics at Oregon State University.

Definition 2.1. *A* convex body *is a compact, convex subset of the plane with nonempty interior.*

More easily, a *convex body* is a set K of points such that the line segment connecting any two points in K does not travel outside of K.

Definition 2.2. *The* directed x-ray *of a set K with respect to an* x-ray source *p is the function* $X_pK : [0, 2\pi] \to \mathbb{R}$ *given by*

$$X_p(\theta) = X_pK(\theta) = \int_0^\infty \chi_K(t(\cos\theta, \sin\theta) + p)dt$$

for $0 \leq \theta \leq 2\pi$*, where* χ_K *is the characteristic function of K.*

As we will be dealing solely with convex bodies in this paper, we can interpret a directed x-ray $X_p(\varphi)$ as the length of the intersection between a ray at angle φ from source *p* and the convex body K.

Definition 2.3. *In this context we will define the* near-side $r_p(\varphi)$ *and* far-side $R_p(\varphi)$ *of an x-ray from source p as the first and second points of intersection, respectively, between the x-ray* $X_p(\varphi)$ *and the boundary of the convex body. When necessary, we shall denote the boundary of a convex body K by* ∂K*.*

Definition 2.4. *By utilizing the notation of Definition 2.3, we may define the x-ray as*

$$X(\varphi) = R(\varphi) - r(\varphi).$$

This provides a mathematical method of finding the x-ray that will be used later in the paper.

Definition 2.5. *The* skew *of a figure from a line is the angle formed between the side of the figure and a ray. In Figure 1,* s_1 *is the near side skew of vertex* v *from ray* φ*,* s_2 *is the far side skew.*

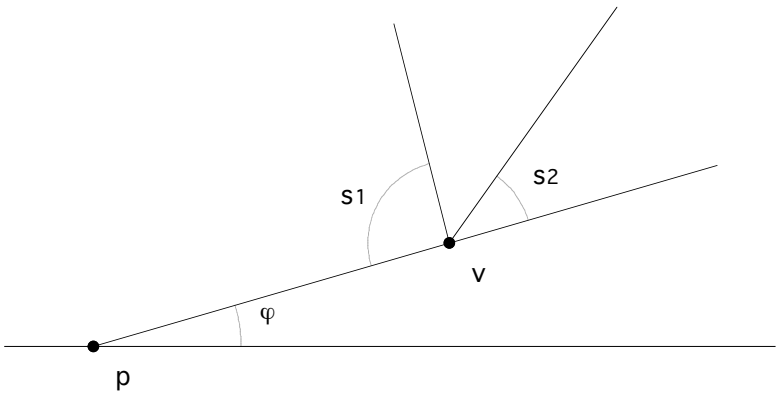

FIGURE 1. Illustration of Definition of Skew

This paper will utilize skew in the statement of theorems concerning angles. It is difficult to describe where these angles exist in words, for a clearer notion of where the angles lie, refer to the figures accompanying each theorem.

Definition 2.6. *The* convex hull *of a set S in the plane,* $\mathrm{ch}(S)$*, is the intersection of all convex sets containing S.*

The triangles and other shapes we will investigate are formed via the convex hull of a set of finite, non-collinear, points.

Definition 2.7. [1] *The curvature operator,* κ*, is*

$$\kappa = f^2 + 2ff' - ff''$$

A postive result shows the function is concave towards the source, a negative result shows concave away.

This will provide an indication whether the figures we investigate are truly convex. It is used in section 5.

2.1. **Preliminary Discussion.**

Theorem 2.8 ([7] Thm 2.4)**.** *Let K be a convex body, p a point source. Suppose* $l_p(\varphi_0)$ *intersects the interior of K. Then* X_pK *is not differentiable at* $\varphi = \varphi_0$ *if and only if at least one of the intersection points of* $l_p(\varphi_0)$ *and* ∂K *is a nonsmooth point of* ∂K*.*

This theorem allows us to identify those x-rays on which a vertex of a figure lies. Clearly, if two figures share the same x-rays, they must also share the same rays on which the vertices of the respective shapes lie. Fithian [4] utilized this fact to analyze the situation regarding a triangle.

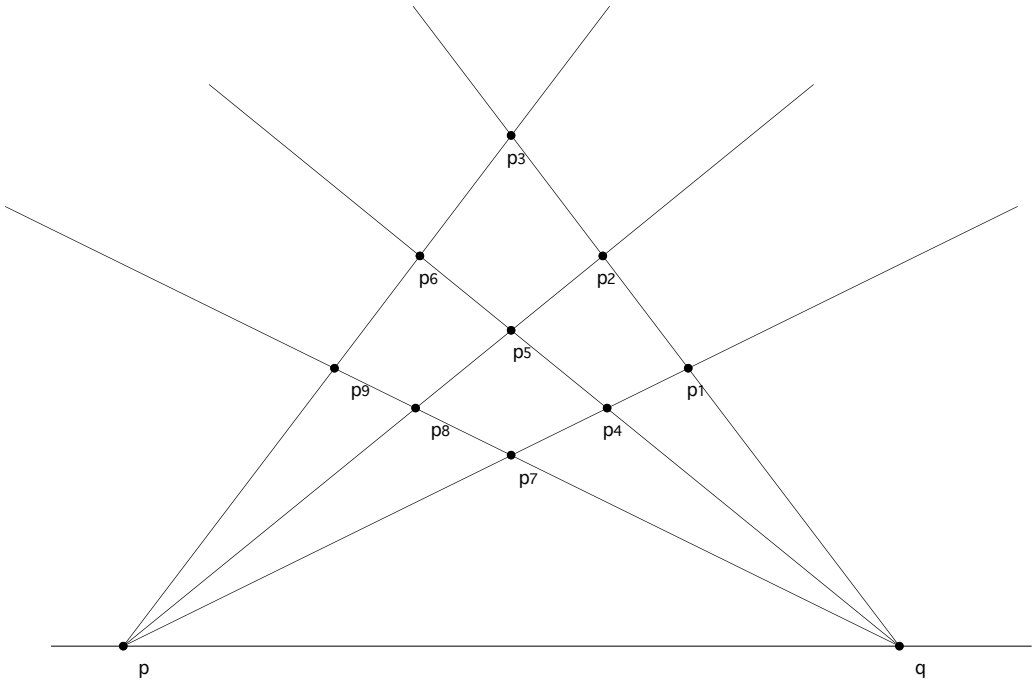

FIGURE 2. Illustration of Vertex Possibilities

A triangle has three vertices; thus there are three (or fewer if two vertices are collinear with a source) x-rays from each source that we can identify as hitting a vertex. This is illustrated in Figure 2. With such a diagram we can pick three points p_j that form the triangle, which I will call the true triangle, for which we know the x-rays. Dependent on that choice, we can pick a set of three other

p_j's, allowing that the intersection of these two selections may not be null, and investigate a body sharing x-rays with the true triangle that has vertices at these three points. I will call the convex hull of these three points the *shadow triangle*. The *shadow body* is the shape sharing x-rays with the true triangle that we are investigating; it necessarily contains the shadow triangle by definition.

In previous work, Fithian [4] eliminated all such combinations of true triangle and shadow triangle vertices except the one shown in Figure 3, corresponding to

$$True\ Triangle\ Vertices = (p_3, p_4, p_8)$$
$$Shadow\ Body\ Vertices = (p_2, p_6, p_7)$$

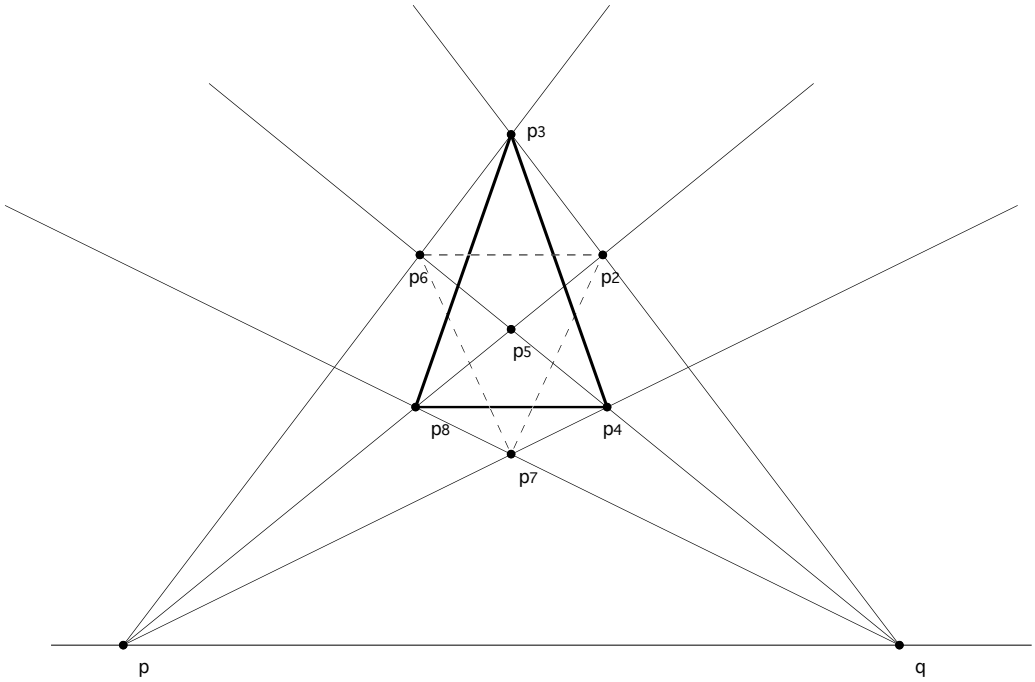

FIGURE 3. Illustration of Remaining Vertex positions

In figure 3 the shadow triangle is shown with dotted outline. We can investigate further points of the shadow body by utilizing the x-ray equality between the shadow body and the true triangle. Referring to Figure 4, the reader can see these newly generated points as Γ and Γ'.

Point Γ is generated by investigating the x-ray $X_p(\varphi_2)$. Since the shadow body shares x-rays with the true triangle, there must exist a point, which we have called Γ, on the boundary of the shadow body at a distance equal to $d(p_8, I1)$. A similar point from source q may be created, which in future diagrams we have called Σ. Γ and Σ lie on the boundary of the shadow body: they are not vertex points like p_2, p_6, or p_7.

The convex hull of the set of five known shadow points, $(\Gamma, \Sigma, p_2, p_6, p_7)$, forms what we will call the shadow pentagon. This pentagon is not necessarily convex; in many cases, point Γ or point Σ is mapped inside of the shadow triangle. The points $(\Gamma, \Sigma, p_2, p_6, p_7)$ must lie on the boundary of a convex body, so if Γ and Σ lie inside the shadow triangle, the shadow body in this configuration will not be convex.

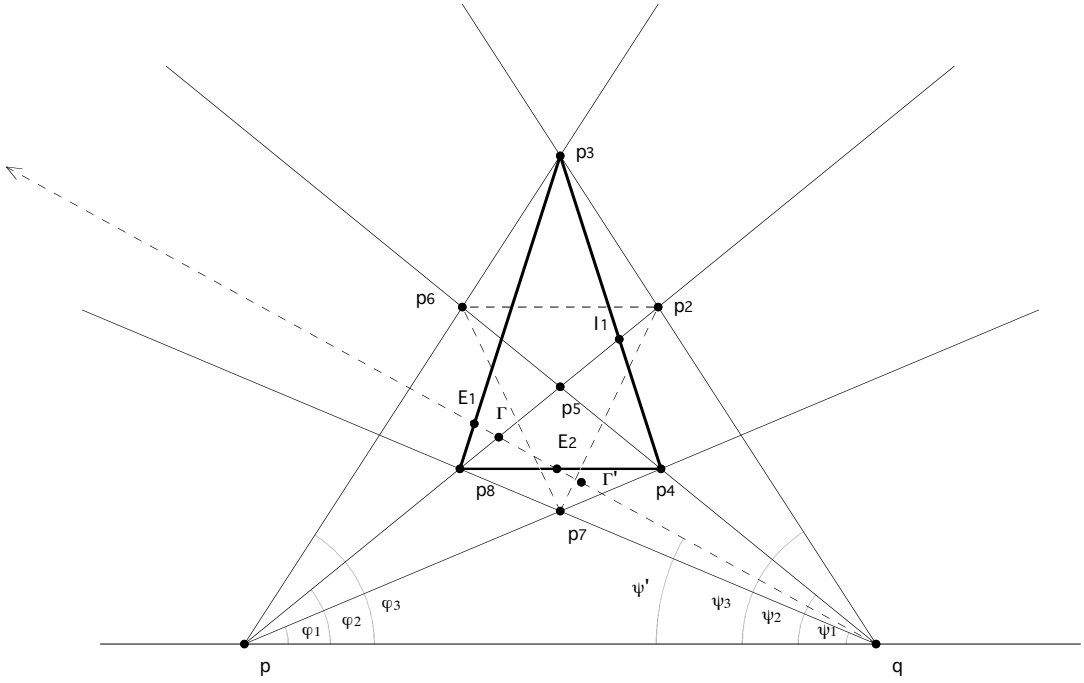

FIGURE 4. Illustration of Method to Obtain Points on ∂K

Further points may be generated via the same method. Point Γ' in Figure 4 is generated by noting that we know Γ lies on the boundary of the shadow body; specifically it lies on the far-side of the shadow body from source q. We can examine the x-ray $X_q(\psi')$ on which Γ lies. There must exist a point, which we have called Γ', at a distance equal to $d(E_1, E_2)$, the x-ray of the true triangle. A companion point, generated the same way from point Σ and source p will be called Σ' later in the paper. As before, there is no promise that these points lie on the boundary of a convex body; the same prohibitions discussed above apply.

More points may be generated by continuing to examine the x-rays passing through Γ' and Σ' from the two x-ray sources. Again, no convexity constraint applies; each new point must be individually investigated as to whether it lies inside the convex hull formed by the previous set of points. At times when such points are needed, they will be denoted by the addition "primes" to Γ and Σ to denote how many repetitions of this process are needed.

Definition 2.9. *At times the paper will use the phrase* switched equivalent. *In regards to an equation, this means that* $\varphi_1 \leftrightarrow \psi_1$, $\varphi_2 \leftrightarrow \psi_2$, *and* $\varphi_3 \leftrightarrow \psi_3$.

This becomes useful later in the paper when we will generate inequalities that work in the presented, and switched equivalent form. For example, distances in Figure 3 are switched equivalents for equivalent sides of triangles. $d(p_7, p_2)$ is the switched equivalent in $d(p_7, p_6)$.

Note. *The computer program* Geometer's Sketchpad *proved invaluable in the investigation of these shapes. Although a program such as Mathematica or Maple can both graphically and numerically duplicate the abilities of* Geometer's Sketchpad, *the time spent configuring them for use greatly outweighs any benefit from slightly more precise calculations; one would not use a hatchet as a butter knife.*

3. Derivative Results

In this section we will examine several results relating to the calculation of derivatives at vertices. These calculations were originally made in order to determine whether the shadow vertex at p_7 could have the correct x-rays from both sources. Regretfully, the equations became too complex to easily compute, but signs pointed to the fact that a vertex could fulfill this requirement.

Lemma 3.1. *In general, the x-ray derivative at angle* φ *is*

$$X'(\varphi) = \lim_{\varphi_1 \to \varphi} \frac{X(\varphi_1) - X(\varphi)}{\sin(\varphi_1 - \varphi)}$$

Proof.

$$X'(\varphi) = \lim_{\varphi_1 \to \varphi} \frac{X(\varphi_1) - X(\varphi)}{\varphi_1 - \varphi}$$

multiplying both sides by $\frac{\sin(\varphi_1-\varphi)}{\sin(\varphi_1-\varphi)}$ shows:

$$= \lim_{\varphi_1 \to \varphi} \frac{\sin(\varphi_1 - \varphi)}{\varphi_1 - \varphi} * \frac{X(\varphi_1) - X(\varphi)}{\sin(\varphi_1 - \varphi)}.$$

The first factor of multiplication equals 1 by simple calculus. □

This lemma will be used in place of the definition of the x-ray derivative in all subsequent calculations. It is considerably easier to compute.

Theorem 3.2. *The x-ray derivative at a vertex* v *lying on a ray at angle* φ *from a source* p *is*

$$X'(\varphi) = d(p,v)\left[\frac{\sin(\omega - \psi)}{\sin(\omega)\sin(\psi)}\right]$$

where ψ *is the near skew from the supporting x-ray* $X(\varphi)$*, and* ω *is the far skew from* $X(\varphi)$*. See Figure 5*

Note. *The form of this proof, heavily dependent on using the Law of Sines to substitute for various quantities and subsequently simplifying, is utilized in almost every proof included in this paper. It is presented without significant omission in the following proof in order to illustrate its form. Subsequent proofs will shield the reader from much of the tedious calculations.*

Proof. Referring to Figure 5, and utilizing the Law of Sines:

$$\frac{L_1}{\sin(\pi - \omega)} = \frac{d(p,v)}{\sin(\omega + \varphi - \varphi)} \qquad \textit{and} \qquad \frac{L_1 + b}{\sin(\pi - \psi)} = \frac{d(p,v)}{\sin(\psi + \varphi - \varphi)}$$

Solving for b, we find:

$$b = d(p,v)\left[\frac{\sin(\pi - \psi)}{\sin(\psi + \varphi_1 - \varphi)} - \frac{\sin(\pi - \omega)}{\sin(\omega + \varphi_1 - \varphi)}\right]$$

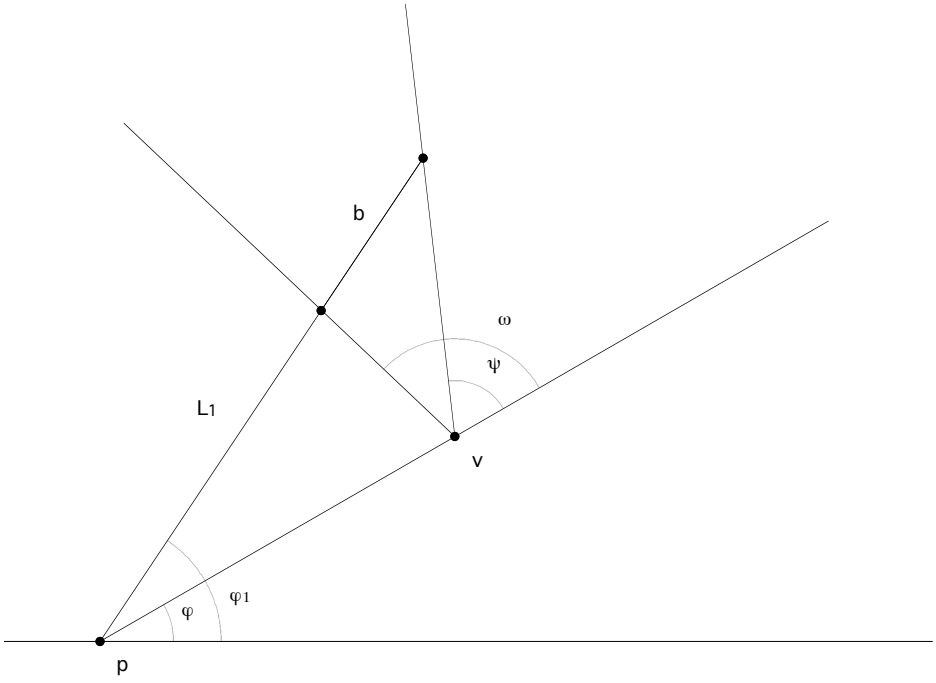

FIGURE 5. Illustration of Derivative Calculation at a Vertex

Utilizing the Sine Addition Formula and simplifying gives:

$$b = d(v,p)\left[\frac{\sin(\omega)\cos(\psi)\sin(\varphi_1-\varphi)-\cos(\omega)\sin(\psi)\sin(\varphi_1-\varphi)}{\sin(\omega+\varphi_1-\varphi)\sin(\psi+\varphi_1-\varphi)}\right]$$

Dividing both sides by $\sin(\varphi_1-\varphi)$ and further simplifying shows that:

$$\frac{b}{\sin(\varphi_1-\varphi)} = d(v,p)\left[\frac{\sin(\omega-\psi)}{\sin(\omega+\varphi_1-\varphi)\sin(\psi+\varphi_1-\varphi)}\right]$$

Taking limits shows

$$\lim_{\varphi_1\to\varphi}\frac{b}{\sin(\varphi_1-\varphi)} = d(v,p)\left[\frac{\sin(\omega-\psi)}{\sin(\omega)\sin(\psi)}\right].$$

As shown in Lemma 3.1,

$$\lim_{\varphi_1\to\varphi}\frac{b}{\sin(\varphi_1-\varphi)} = X'(\varphi).$$

yielding

$$X'(\varphi) = d(p,v)\left[\frac{\sin(\omega-\psi)}{\sin(\omega)\sin(\psi)}\right].$$

□

Remark. *It is important to note that a vertex will have the same derivative if the lines composing the sides of the vertex are extended past the supporting X-ray, and the X-rays approach the vertex from below instead of from above. This situation is illustrated, in the simple case of the vertex lying on the horizontal, below:*

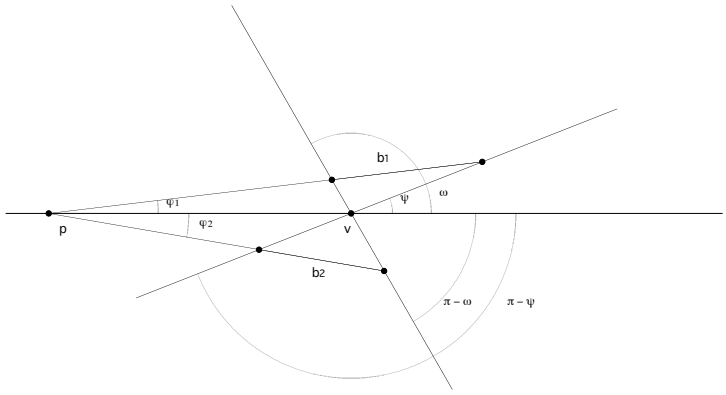

FIGURE 6. Illustration of Equal Derivatives on Either Side of Vertex

This fact is easily seen analytically.
Derivative at 0:

$$X'(0) = \lim_{\varphi_1 \to \varphi} \frac{X(\varphi_1) - X(0))}{\sin(\varphi_1 - 0)}$$

Upper Derivative at 0:

$$X'_+(0) = \lim_{\varphi_1 \downarrow \varphi} \frac{X(\varphi_1) - X(0))}{\sin(\varphi_1 - 0)}$$

Lower Derivative at 0:

$$X'_-(0) = \lim_{\varphi_2 \uparrow \varphi} \frac{X(\varphi_2) - X(0))}{\sin(\varphi_2 - 0)}$$

We know the upper derivative

$$X'_+(0) = \lim_{\varphi_1 \downarrow 0} \frac{b_1}{\sin(\varphi_1 - 0)} = d(p,v) \left[\frac{\sin(\omega - \psi)}{\sin(\omega)\sin(\psi)} \right].$$

Calculating the lower derivative shows

$$X'_-(0) = \lim_{\varphi_2 \uparrow 0} \frac{b_2}{\sin(\varphi_2 - 0)} = d(p,v) \left[\frac{\sin((\pi - \omega) - (\pi - \psi))}{\sin(\pi - \omega)\sin(\pi - \psi)} \right] = d(p,v) \left[\frac{\sin(-\omega + \psi)}{\sin(\omega)\sin(\psi)} \right].$$

This result is important as many systems of equations later in the paper will, when solved, turn into quadratic forms with 2 solutions. This remark provides a context in which to interpret such solutions and pick the appropriate one.

Lemma 3.3. *The derivative at a vertex* v *from a second x-ray source in terms of the angles from the first will equal*

$$X_q'(\varphi_2) = d(p,v)\left[\frac{\sin(\varphi_1)\sin(\omega_1-\psi_1)}{\sin(\varphi_2)\sin(\varphi_1+\varphi_2+\omega_1)\sin(\varphi_1+\varphi_2+\psi_1)}\right]$$

with ψ_1, ω_1 *defined as in Theorem 3.2 as coming from the original X-ray source.* φ_1 *and* φ_2 *are the angles of support of the vertex* v *from the first and second sources (p and q), respectively.*

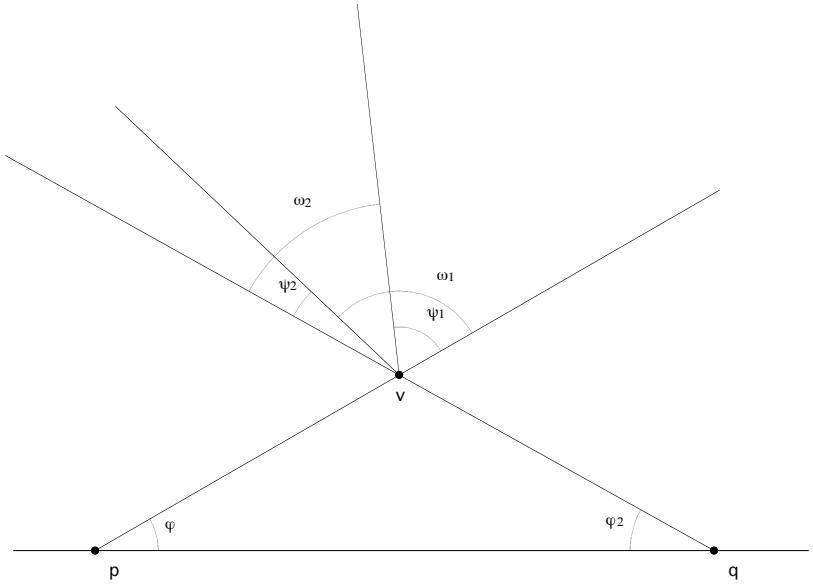

FIGURE 7. Illustration of Derivative Relationship

Proof. Utilizing Theorem 3.2 we see that the two derivatives are

$$X_p'(\varphi_1) = d(p,v)\left[\frac{\sin(\omega_1-\psi_1)}{\sin(\omega_1)\sin(\psi_1)}\right] \text{ and } X_q'(\varphi_2) = d(p,v)\left[\frac{\sin(\omega_2-\psi_2)}{\sin(\omega_2)\sin(\psi_2)}\right].$$

Apply the Law of Sines to solve d(q,v) in terms of d(p,v) and notice, referring to Figure 7

$$\psi_2 = \pi-\varphi_1-\varphi_2-\omega_1 \text{ and } \omega_2 = \pi-\varphi_1-\varphi_2-\psi_1.$$

□

Theorem 3.2 provides an easy way to compute the x-ray derivative at a vertex. Clearly, there must be equality between the derivative of the shadow body at the vertex at p_7 and the derivatives of the true triangle from both sources. The next theorem shows that useful information at vertex p_7 may be gained by the investigation of this relationship. Modification of the previous derivative theorems would provide similar information for the shadow vertices at p_2 and p_8. These relationships would prove more complex due to the geometry of the figures, and thus are left for future work.

Theorem 3.4. *The x-ray derivative at an angle* φ_1 *from a source* p *is*

$$X'(\varphi_1) = d(p,v)\sin(\omega-\psi)*$$
$$\left[\frac{\cos(\omega-(\varphi_1-\varphi))\sin(\varphi_1-\varphi)\sin(\psi-(\varphi_1-\varphi))+\sin(\psi)\sin(\omega-(\varphi_1-\varphi))}{\sin(\omega-(\varphi_1-\varphi))^2\sin(\psi-(\varphi_1-\varphi))^2}\right]$$

where ψ *is the near skew from the supporting x-ray* $X(\varphi)$ *of the vertex* v*, and* ω *is the far skew from* $X(\varphi)$*. See Figure 8*

Corollary 3.5. *The x-ray second derivative at a vertex* v *lying on a ray at angle* φ *from a source* p *is*

$$X''(\varphi) = -d(p,v)\left[\frac{(\cos(2\omega)-\cos(2\psi))}{\sin(\omega)^2\sin(\psi)^2}\right]$$

where ψ *is the near skew from the supporting x-ray* $X(\varphi)$*, and* ω *is the far skew from* $X(\varphi)$*. See Figure 8*

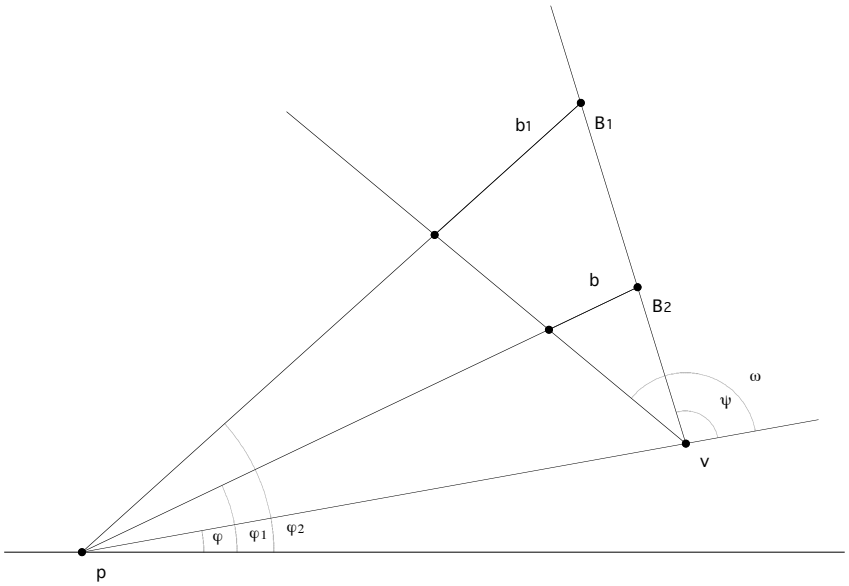

FIGURE 8. Illustration of Derivative Relationship Not At Vertex

Proof. Solve for b_1 and b in Figure 8:

$$b_1 = \frac{d(p,v)\sin(\omega-\psi)\sin(\varphi_2-\varphi)}{\sin(\omega-(\varphi_2-\varphi))\sin(\psi-(\varphi_2-\varphi))} \qquad \textit{and} \qquad b = \frac{d(p,v)\sin(\omega-\psi)\sin(\varphi_1-\varphi)}{\sin(\omega-(\varphi_1-\varphi))\sin(\psi-(\varphi_1-\varphi))}.$$

Then

$$b_1 - b = d(p,v)\sin(\omega-\psi)*$$
$$\frac{\sin(\varphi_2-\varphi)\sin(\omega-(\varphi_1-\varphi))\sin(\psi-(\varphi_1-\varphi))-\sin(\varphi_1-\varphi)\sin(\omega-(\varphi_2-\varphi))\sin(\psi-(\varphi_2-\varphi))}{\sin(\omega-(\varphi_2-\varphi))\sin(\omega-(\varphi_1-\varphi))\sin(\psi-(\varphi_2-\varphi))\sin(\psi-(\varphi_1-\varphi))}.$$

Dividing both sides by $\sin\varphi_2 - \varphi_1$, taking the limit $\lim_{\varphi_2 \to \varphi_1}$ and utilizing geometric identities yields the theorem.

The corollary is proved by using Theorems 3.2 and 3.4 to compute

$$\lim_{\varphi_1 \to \varphi} \frac{X'(\varphi_1) - X'(\varphi)}{\sin(\varphi_1 - \varphi)}.$$

□

This corollary will see use in Section 5.

Note. *It will be helpful that the reader fully understands the method for solving for the tangent of angles that is used in the following examples and elsewhere. While it would be best to solve for an angle explicitly, that would not always result in the cleanest calculation. Angles have been left in the implicit form of* $\tan(angle)$ *for the ease of the reader.*

Solving for angles reliant upon angles of either triangle requires a lengthy Law of Sines calculation. In general, the first such relation will take the form

$$\frac{D_1}{\sin(x)} = \frac{D_2}{\sin(\pi - x - \varphi_j - \psi_k)},$$

where x is the angle to be solved for, and D_1, D_2 *distances. Cross multiplication and expansion of the* $\sin(\pi - x - \varphi_j - \psi_k)$ *term follows*

$$D_2 \sin(x) = D_1 \left(\sin(x)\cos(\varphi_j + \psi_k) + \cos(x)\sin(\varphi_j + \psi_k)\right).$$

One then has the choice of dividing through by $\cos(x)$ *or* $\sin(x)$*. The latter gives a solution for* $\cot(x)$*, the former the more common* $\tan(x)$ *function. Division and simplification yields*

$$\tan(x) = \frac{D_1 \sin(\varphi_j + \psi_k)}{D_2 - D_1 \cos(\varphi_j + \psi_k)}.$$

Example 3.6. *We will now calculate parts of the angles* ψ *and* ω *utilized in the derivative calculation of Theorem 3.2 at vertex* p_2*. This will be useful as an example of the angle solving techniques utilized throughout the paper, as well as provide numerical answers for these angles later.*

Call the two angles we are calculating α *and* ψ^s *for clarity. Referring to Figure 9, we begin the calculation of* ψ^s

$$d(p_4, p_1)\sin(\psi^s) = d(p_1, p_3)\sin(\psi^s + \varphi_1 + \psi_3),$$

then

$$\tan(\psi^s) = \frac{d(p_1, p_3)\sin(\varphi_1 + \psi_3)}{d(p_4, p_1) - d(p_1, p_3)\cos(\psi_1 + \psi_3)}.$$

The Law of Sines allows both $d(p_1, p_3)$ *and* $d(p_4, p_1)$ *to be solved in terms of* $d(p, q)$*. With cancellation and simplification*

$$\tan(\psi^s) = \frac{\sin(\psi_3)\sin(\varphi_3 - \varphi_1)\sin(\varphi_1 + \psi_2)\sin(\varphi_1 + \psi_3)}{\sin(\varphi_1)\sin(\psi_3 - \psi_2)\sin(\varphi_3 + \psi_3) - \sin(\psi_3)\sin(\varphi_3 - \varphi_1)\sin(\varphi_1 + \psi_2)\cos(\varphi_1 + \psi_3)}.$$

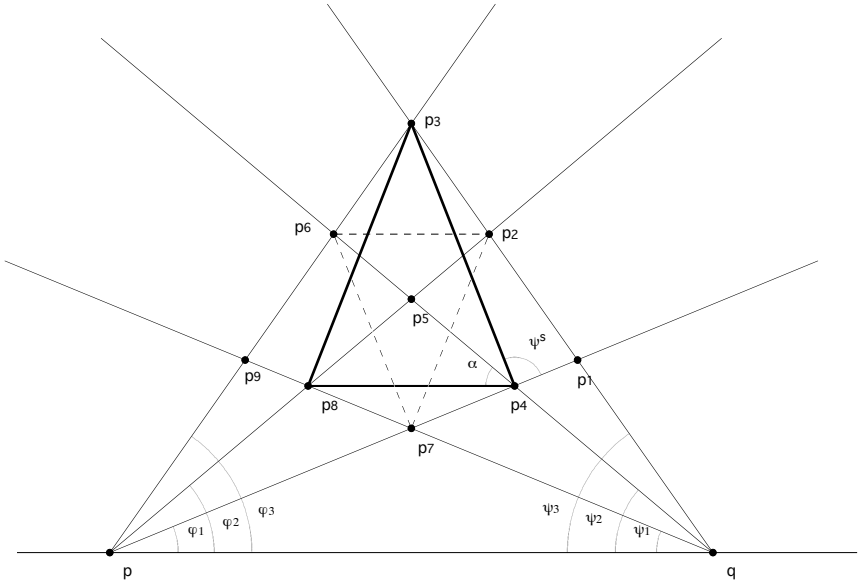

FIGURE 9. Illustration of Angles ψ^s and α

The same method gives the solution for $\tan(\alpha)$

$$\tan(\alpha) = \frac{\sin(\psi_2-\psi_1)\sin(\varphi_2)\sin(\varphi_2+\psi_2)}{\sin(\varphi_2-\varphi_1)\sin(\psi_2)\sin(\varphi_2+\psi_2)-\sin(\psi_2-\psi_1)\sin(\varphi_2)\sin(\varphi_1+\psi_2)\cos(\varphi_2+\psi_2)}.$$

Theorem 3.7. *The skew from the horizontal and interior angle of the tangent lines at a vertex are found by solving*

$$\frac{d(p,q)\sin(\psi)\sin(\alpha)}{\sin(\varphi+\psi)\sin(s_1+\varphi+\alpha)\sin(s_1+\varphi)} - X_p'(\varphi) = 0$$

and

$$\frac{d(p,q)\sin(\varphi)\sin(\alpha)}{\sin(\varphi+\psi)\sin(s_1-\psi)\sin(s_1+\alpha-\psi)} - X_q'(\psi) = 0$$

for s_1*, representing skew from the horizontal of the supporting ray to the vertex from the leftmost source and* α*, the interior angle of the tangent lines. See Figure 10.*

Proof. Referring to 10 and utilizing the Law of Sines, we solve for b_1 and b_2 in terms of $d(p,q)$, obtaining:

$$b_1 = \frac{d(p,q)\sin(\psi)\sin(\varphi_1-\varphi)\sin(\alpha)}{\sin(\pi-\varphi-\psi)\sin(\pi-s_1-\varphi_1-\alpha)\sin(\varphi_1+s_1)}$$

and

$$b_2 = \frac{d(p,q)\sin(\varphi)\sin(\psi_1-\psi)\sin(\alpha)}{\sin(\pi-\varphi-\psi)\sin(\pi-s_2-\psi_1-\alpha)\sin(\psi_1+s_2)}.$$

Dividing b_1 by $\sin(\varphi_1-\varphi)$ and b_2 by $\sin(\psi_1-\psi)$ and taking the limits yields:

$$X_p'(\varphi) = \frac{d(p,q)\sin(\psi)\sin(\alpha)}{\sin(\varphi+\psi)\sin(s_1+\varphi+\alpha)\sin(s_1+\varphi)}$$

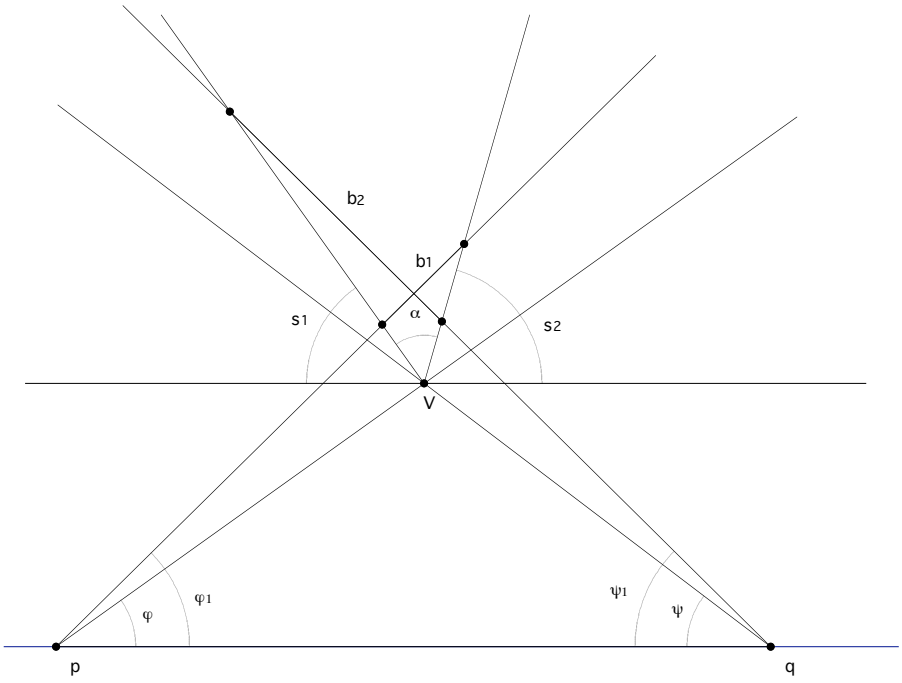

FIGURE 10. Illustration of Derivative Calculation

and

$$X_q'(\psi) = \frac{d(p,q)\sin(\varphi)\sin(\alpha)}{\sin(\varphi+\psi)\sin(s_2+\psi+\alpha)\sin(\psi+s_2)}.$$

Utilizing the identity $s_2 = \pi - s_1 - \alpha$ shows the second equation is equivalent to

$$X_q'(\psi) = \frac{d(p,q)\sin(\varphi)\sin(\alpha)}{\sin(\varphi+\psi)\sin(s_1-\psi)\sin(s_1+\alpha-\psi)}$$

□

This theorem shows that partial reconstruction of the shadow body may not be as difficult as previously thought. While the information about a single vertex does not help prove existence or non-existence of a convex shadow body, this theorem would provide a starting point to many avenues of investigation. Further work pointed to the existence of the shadow body in a specialized situation where easier computations are available.

Theorem 3.8. *The derivatives of the lowest vertex of the convex pentagon M, formed by including the points* Γ *and* Σ *in the triangle diagram are*

$$X_p'(\varphi_1) = \frac{\sin(\pi-\varphi_1-\psi_1-j-j')}{\sin(\pi-\varphi_1-\psi_1-j)\sin(j')}$$

and

$$X_q'(\psi_1) = \frac{\sin(\pi-\varphi_1-\psi_1-j'-j)}{\sin(\pi-\varphi_1-\psi_1-j')\sin(j)}.$$

where the angles j, j', k, k' *are described below and shown in Figure 12.*

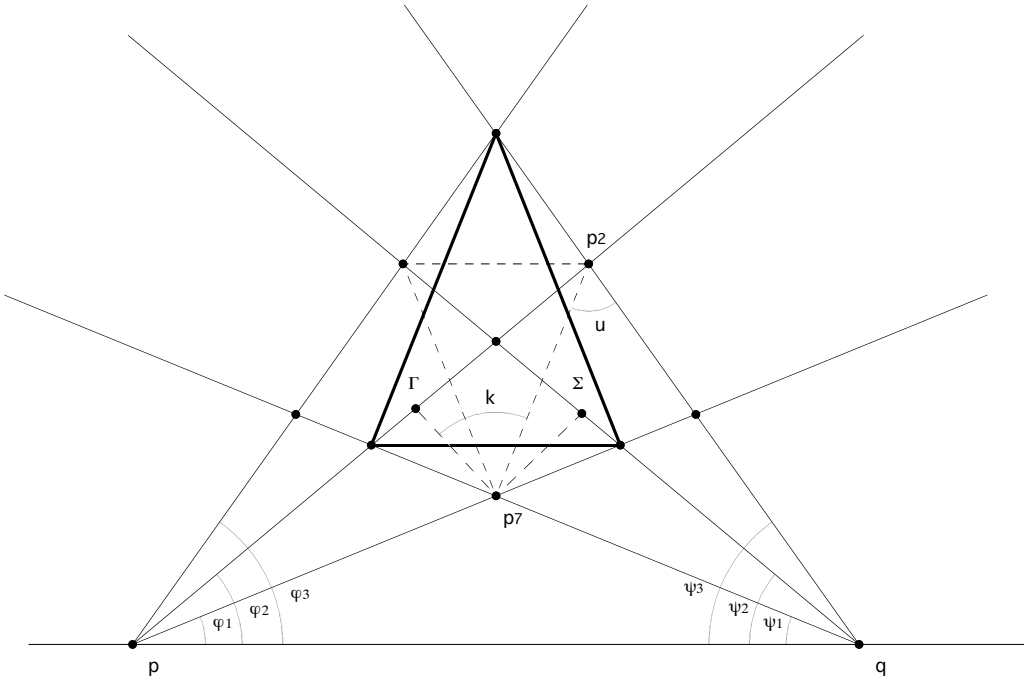

FIGURE 11. Illustration of Pentagon Derivative Calculation

Proof. Our final goal is to determine angles *j, j', k, k'* as shown in Figure 12. In order to do so, several other quantities must be calculated beforehand. These terms will remain in un-expanded form so as not to complicate the paper needlessly.
Our first step is to find $d(p_2, p_7)$ as seen in figure 11; this requires a calculation of angle u. The Law of Sines solves for both the distance and the angle as

$$\tan(u) = \frac{\sin(\varphi_1)\sin(\psi_3+\psi_1)\sin(\varphi_2+\psi_3)}{\sin(\varphi_2)\sin(\varphi_1+\psi_1)-\sin(\varphi_1)\sin(\varphi_2+\psi_3)\cos(\psi_3+\psi_1)}$$

and

$$d(p_2, p_7) = \frac{d(p,q)\sin(\varphi_2)\sin(\psi_3-\psi_1)}{\sin(\varphi_2+\psi_3)\sin(\psi_3+\psi_1+u)}.$$

$d(\Gamma, p2)$ is, by definition, equal to the X-ray length through vertex p_7. This distance is computed in Theorem 4.1, where its derivation is examined in more depth. Its formula is reproduced here for ease of reading.

$$X'_p(\varphi_2) = \frac{(d(p,q)\sin(\psi_2)\sin(\varphi_2-\varphi_1)\sin(c)}{\sin(\varphi_2+\psi_2)\sin(\varphi_1+\psi_2)\sin(\varphi_2+\psi_2+c)} + \frac{d(p,q)\sin(\varphi_2)\sin(\psi_2-\psi_1)}{\sin(\varphi_2-\psi_1)\sin(\varphi_2+\psi_2)}$$

with

$$\sin(c) = \sin(\varphi_3)\sin(\psi_3-\psi_2)\sin(\varphi_3+\psi_2)\sin(\varphi_1+\psi_2)$$

and

$$\cos(c) = \sin(\psi_2)\sin(\varphi_3-\varphi_1)\sin(\varphi_3+\psi_3) - \sin(\varphi_3)\sin(\psi_3-\psi_2)\sin(\varphi_1+\psi_2)\cos(\varphi_3+\psi_2).$$

We can now use the Law of Sines to calculate angle k:

$$\tan(k) = \frac{d(\Gamma, p2)\sin(\varphi_2+\psi_3+u)}{d(p_7,p_2) - d(\Gamma,p2)\cos(\varphi_2+\psi_3+u)}.$$

Examining Figure 12 shows that angle $e = \pi - \varphi_2 - \psi_3 - u$. This then allows us to solve for angle j:

$$j = \psi_3 - \psi_1 + u - k.$$

As in other proofs in this paper, examination of the situation in Figure 12 allows us to see that *k'* and *j'* are mirror images of k and j. This means their calculation requires only a replacement of a φ angle with the corresponding ψ angle. Utilizing Theorem 3.2 concludes the proof. □

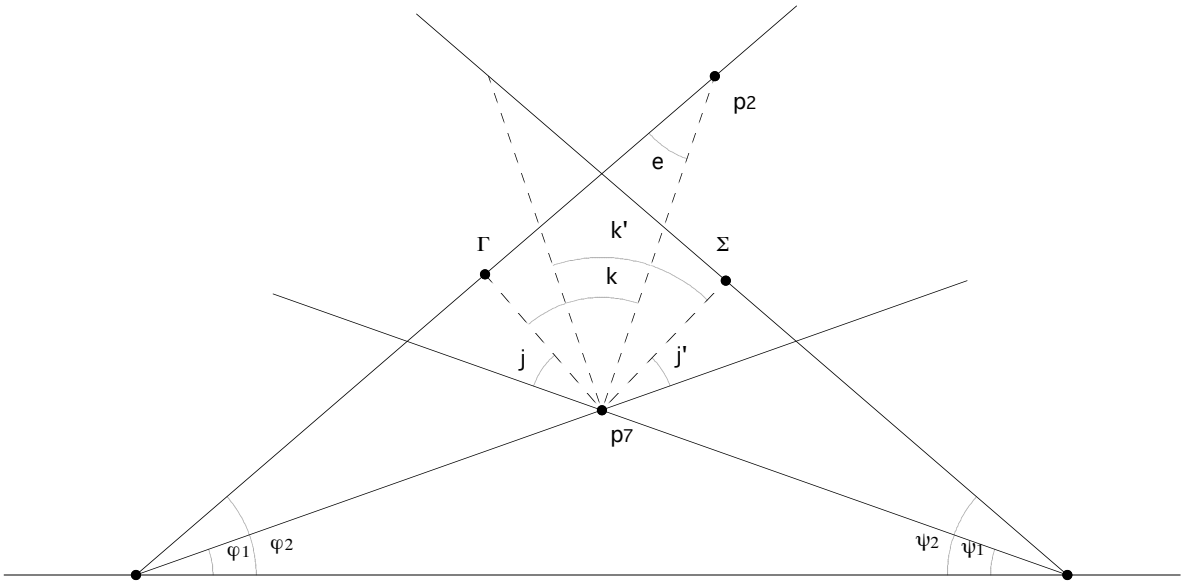

FIGURE 12. Close-Up of Pentagon Derivative Calculations

4. DISTANCE RESULTS

Direct computation of the angles involved in the shadow triangle and shadow pentagon quickly became difficult. Fithian [4] computed 100,000 random examples, and in each case points Γ' and Σ' would lie inside the shadow pentagon leading to a contradiction. (The shadow figure formed by the collection of seven known points on the boundary of the shadow figure would not be convex). Theorem 4.1 derives a condition necessary for this convexity, and work was made to determine whether Γ' and Σ' could exist while fulfilling this condition. Numerically, an inconsequential solution was found. *Geometer's Sketchpad* showed many solutions, and indicated the existence of further points in certain configurations. A general form of these configurations is examined in Section 5.

Theorem 4.1. *For* Γ *and* Σ *to exist (and thus form a convex shadow pentagon), the following inequality, and its switched equivalent, must hold:*

$$\frac{\sin(\psi_2)\sin(\varphi_2-\varphi_1)\sin(k_2)}{\sin(\varphi_1+\psi_2)\sin(\varphi_2+\psi_2+k_2)}+\frac{\sin(\varphi_2)\sin(\psi_2-\psi_1)}{\sin(\varphi_2+\psi_1)}$$

$$>$$

$$\frac{\sin(\psi_2)\sin(\varphi_3-\varphi_2)\sin(k_1)}{\sin(\varphi_3+\psi_2)\sin(\varphi_2+\psi_2+k_1)}+\frac{\sin(\varphi_2)\sin(\psi_3-\psi_2)}{\sin(\varphi_2+\psi_3)},$$

where

$$\sin(k_2)=\sin(\varphi_3)\sin(\psi_3-\psi_2)\sin(\varphi_3+\psi_2)\sin(\varphi_1+\psi_2),$$
$$\cos(k_2)=\sin(\psi_2)\sin(\varphi_3-\varphi_1)\sin(\varphi_3-\psi_3)-\sin(\varphi_3)\sin(\psi_3-\psi_2)\sin(\varphi_1+\psi_2)\cos(\varphi_3+\psi_2),$$

$$\sin(k_1)=\sin(\varphi_1)\sin(\psi_2-\psi_1)\sin(\varphi_3+\psi_2)\sin(\varphi_1+\psi_2),$$
$$\cos(k_1)=\sin(\psi_2)\sin(\varphi_3-\varphi_1)\sin(\varphi_1+\psi_1)-\sin(\varphi_1)\sin(\psi_2-\psi_1)\sin(\varphi_3+\psi_2)\cos(\varphi_1+\psi_2).$$

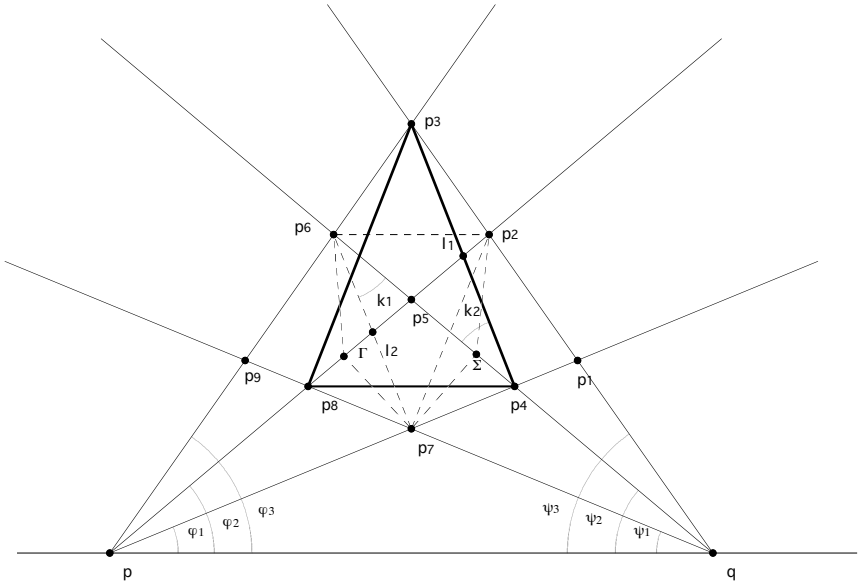

FIGURE 13. Gamma and Sigma Existence

Proof. We will derive the inequality for a single side of the shape; that is we will derive the inequality required for the existence of Γ alone. As can be seen in Figure 13, the existence of Σ will depend on exactly the same rays as the existence of Γ although every φ_j will be switched to its ψ_j equivalent and vice-versa.

The existence of Γ depends on the lengths of $d(p_8,I_1)$ and $d(I_2,p_2)$. Namely, the following must be satisfied:

$$d(p_8,I_1)>d(I_2,p_2).$$

Otherwise Γ will be located inside the shadow triangle, thus making the shadow body non-convex. The inequality above breaks into

$$d(p_8,p_5)+d(p_5,I_1)>d(p_2,p_5)+d(p_5,I_2).$$

Both $d(p_8,p_5)$ and $d(p_2,p_5)$ are easy to find via the Law of Sines, so we will ignore them for the time being. Calculation of $d(p_5,I_1)$ requires the calculation of angle k_2. We find:

$$d(p_5,I_1)=\frac{\sin(\psi_2)\sin(\varphi_2-\varphi_1)\sin(k_2)}{\sin(\varphi_1+\psi_2)\sin(\varphi_2+\psi_2+k_2)}$$

and

$$\tan(k_2)=\frac{\sin(\varphi_3)\sin(\psi_3-\psi_2)\sin(\varphi_3+\psi_2)\sin(\varphi_1+\psi_2)}{\sin(\psi_2)\sin(\varphi_3-\varphi_1)\sin(\varphi_3-\psi_3)-\sin(\varphi_3)\sin(\psi_3-\psi_2)\sin(\varphi_1+\psi_2)\cos(\varphi_3+\psi_2)}.$$

Similarly, $d(p_5,I_2)$ requires angle k_1:

$$d(p_5,I_2)=\frac{\sin(\psi_2)\sin(\varphi_3-\varphi_2)\sin(k_1)}{\sin(\varphi_3+\psi_2)\sin(\varphi_2+\psi_2+k_1)}$$

and

$$\tan(k_1)=\frac{\sin(\varphi_1)\sin(\psi_2-\psi_1)\sin(\varphi_3+\psi_2)\sin(\varphi_1+\psi_2)}{\sin(\psi_2)\sin(\varphi_3-\varphi_1)\sin(\varphi_1+\psi_1)-\sin(\varphi_1)\sin(\psi_2-\psi_1)\sin(\varphi_3+\psi_2)\cos(\varphi_1+\psi_2)}.$$

Clearly, $d(p_5,I_1)$ and $d(p_5,I_2)$ contain terms of sine involving their respective angles in both numerator and denominator. This allows us to use the numerator of the tangent calculation as sine and the denominator as cosine.

The Law of Sines shows

$$d(p_8,p_5)=\frac{\sin(\varphi_2)\sin(\psi_2-\psi_1)}{\sin(\varphi_2+\psi_1)}$$

and

$$d(p_2,p_5)=\frac{\sin(\varphi_2)\sin(\psi_3-\psi_2)}{\sin(\varphi_2+\psi_3)}.$$

Substitution yields the desired inequality. □

Numerical computation both by Fithian [4] and myself proved that this condition was satisfied in a multitude of situations. Although the inequality does not factor nicely, graphical representation indicates an interpretation that the figures formed by the set of p_j points may not be too skewed from between the two sources and still have a convex shadow pentagon. Thus the closer both the true and shadow triangles formed resemble isosceles triangles, the more freedom is allowed the vertex rays while still satisfying this inequality.

4.1. **Computations For Γ' and Σ'.** The next step was to compute an inequality for the existence of Γ' and Σ'. At the outset of this multi-step computation, I believed that I could find a simple way of relating the distances interior to the true and shadow triangles to show non-existence. The inequality that is the final result of these calculations is not simple to find solutions for, and was cast aside when graphical analysis via *Geometer's Sketchpad* proved the existence of Γ' and Σ' in certain situations.

The final inequality of this section is the composition of several parts that are most easily computed separately. Each of these parts is presented as a separate lemma as they may prove useful in future calculations; as well as the fact they are computationally intensive and best computed separately.

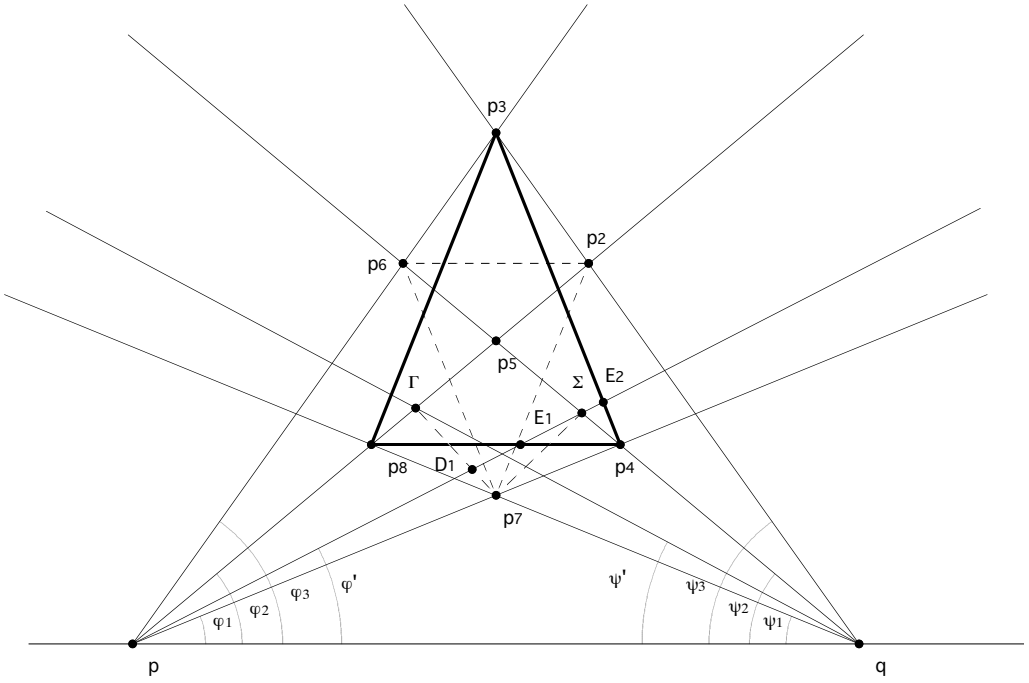

FIGURE 14. Illustration of Distance to Γ' Calculation

Theorem 4.2. *Assume the shadow pentagon defined by points* Γ *and* Σ *is convex. Let* $X_p(\varphi')$ *be the x-ray from source* p *intersecting* Σ *and* $X_q(\psi')$ *be its equivalent from source q to* Γ *as in Figure 14. Then the following inequality must hold so that point* Γ' *is mapped outside of the shadow pentagon (and thus we retain convexity of the shadow body). The switched equivalent of the theorem will provide the condition for convexity with point* Σ'.

$$\frac{\sin(\varphi_2+\psi_3)}{\sin(\psi_3-\psi')\sin(\varphi'+\varphi'\sin(\varphi_2)}*$$

$$\left(\frac{\sin(\psi')\sin(\varphi_2+\psi'+B_1)\sin(\varphi_2-\varphi')}{\sin(\varphi_2-\varphi'+B_1)}+\frac{\sin(\psi_2-\psi')\sin(\varphi_2+\psi')\sin(\varphi')}{\sin(\varphi'+\psi_2)}\right)$$

$$>$$

$$\frac{\sin(\varphi_2+s)\sin(\varphi'-\varphi_1)\sin(s+\alpha+(\varphi_2-\varphi_1))}{\sin(\varphi'+s)\sin(\varphi_2-\varphi_1)\sin(s+\alpha+(\varphi'-\varphi_1))}.$$

where angles s, α*, and* $s+\alpha$ *have the following values*

$$\tan(s)=\frac{\sin(\psi_1)\sin(\varphi_2-\varphi_1)\sin(\varphi_1+\psi_2)}{\sin(\psi_2)\sin(\varphi_2+\psi_1)-\sin(\psi_1)\sin(\varphi_1+\psi_2)\cos(\varphi_2-\varphi_1)}$$

and

$$\tan(s+\alpha)=$$
$$Numerator=\sin(\varphi_2-\varphi_1)\sin(\varphi_1+\psi_2)(\sin(\varphi_2)\sin(\psi_3-\psi')\sin(\varphi_2+\psi_1+\sin(\psi_1)$$
$$*\sin(\varphi_2+\psi_3)\sin(\varphi_2+\psi')$$
$$Denominator=\sin(\psi_2)\sin(\varphi_2+\psi_3)\sin(\varphi_2+\psi')\sin(\varphi_2+\psi_1)$$
$$-\sin(\varphi_1+\psi_2)\cos(\varphi_2-\varphi_1)(\sin(\varphi_2)\sin(\psi_3-\psi')\sin(\varphi_2+\psi_1)+\sin(\psi_1)\sin(\varphi_2+\psi_3)\sin(\varphi_2+\psi')$$

and

$$\tan(B_1)=\frac{\sin(\varphi_2-\varphi_1)\sin(\psi_1)\sin(\varphi_2+\psi')}{\sin(\psi')\sin(\varphi_1+\psi_1)-\sin(\psi_1)\sin(\varphi_2+\psi')\cos(\varphi_2-\varphi_1)}.$$

s *is the skew of the vertex at* p_4*, and* α *the measure of the angle of the true triangle at that vertex. Both angles, and angle* B_1 *are shown in Figure 18.*

Proof. As stated previously, this proof will be divided into separate lemmas.

Lemma 4.3. *Let* b_1 *and* b_2 *be two x-rays, from a single source of a figure with straight sides. If* φ_2 *is the angle from the horizontal for* b_1 *and* φ' *for* b_2*, and* $\varphi_2>\varphi'$*,* $b_1>b_2$*, then* b_1 *and* b_2 *are related by the formula*

$$b_2=\frac{b_1\sin(\varphi_2+s)\sin(\varphi'-\varphi_1)\sin(s+\alpha+(\varphi_2-\varphi_1))}{\sin(\varphi'+s)\sin(\varphi_2-\varphi_1)\sin(s+\alpha+(\varphi'-\varphi_1))}$$

where s is the skew of the vertex from the supporting ray φ_1 *and* α *is is the angle of said vertex.*

Proof. Examination of Figure 15 and the Law of Sines provides the necessary information.

$$\frac{b_1}{\sin(\alpha)}=\frac{d(B_1,v)}{\sin(\varphi_2+s)}\qquad and\qquad \frac{b_2}{\sin(\alpha)}=\frac{d(B_2,v)}{\sin(\varphi'+s)}.$$

Solving for $d(p,v)$ in b_1's Law of Sine equations gives

$$d(p,v)=\frac{b_1\sin(s+\alpha+(\varphi_2-\varphi_1)\sin(\varphi_2+s)}{\sin(\alpha)\sin(\varphi_2-\varphi_1)}.$$

Substituting this back into the equation for b_2 gives the theorem. □

This theorem has obvious importance in calculating how far points must be from each other. While it is not currently used further in this paper, it will be useful in further calculations of points Γ'', Σ'', etc.

Lemma 4.4. *The length of segment* L *in Figure 16 in terms of* $d(A,B)$ *is*

$$d(L)=\frac{d(A,B)\sin(\varphi_1+\psi)\sin(\psi_1)\sin(\varphi_1+\psi_1+B_1)\sin(\varphi_1-\varphi')}{\sin(\psi_1-\psi)\sin(\varphi_1)\sin(\varphi'+\varphi_1)\sin((\varphi_1-\varphi')+B_1}.$$

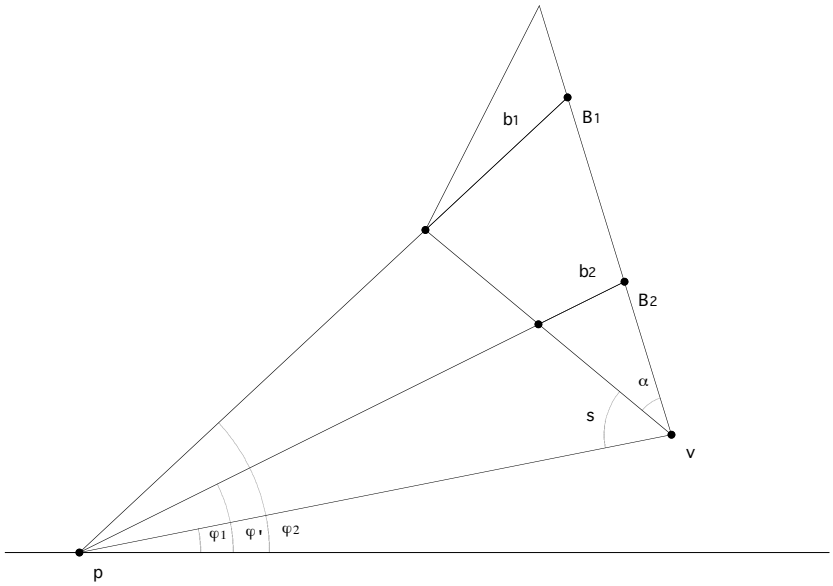

FIGURE 15. Illustration of X-Ray Distance Relationship

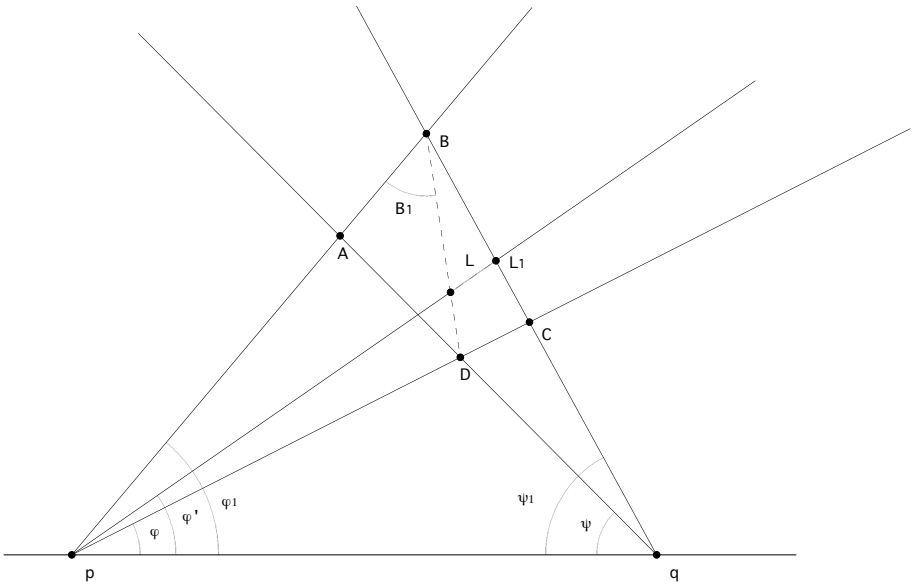

FIGURE 16. Illustration of Quadrilateral Diagonal Segment Calculation

Proof. This is an elementary Law of Sines calculation for $d(L)$. Solving for angle B_1 will wait until the lemma is utilized in its specific location later in the proof of Theorem 4.2. □

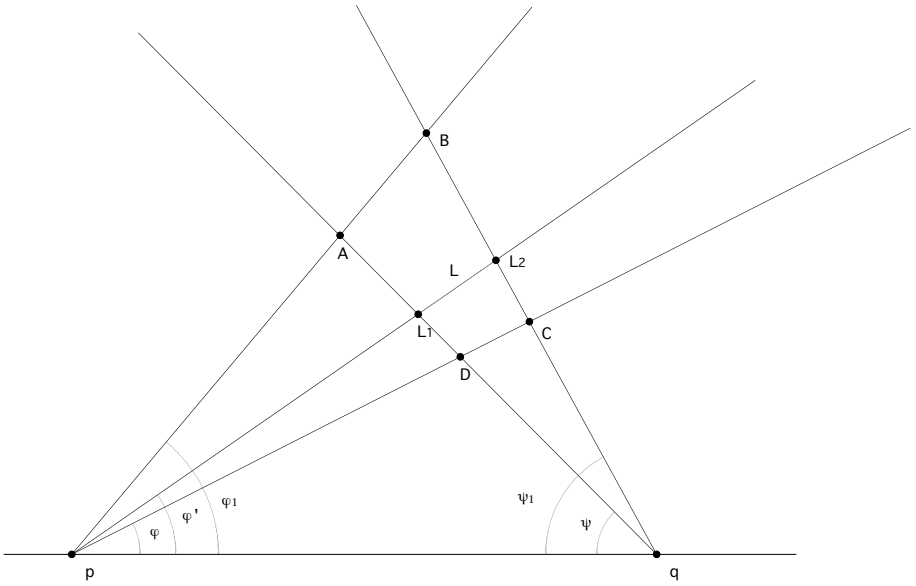

FIGURE 17. Illustration of Quadrilateral Side Calculation

Lemma 4.5. *The length of* L *in Figure 17 in terms of* $d(A,B)$ *is*

$$L = \frac{d(A,B)\sin(\varphi_1+\psi_1)\sin(\varphi_1+\psi)\sin(\varphi')}{\sin(\varphi'+\psi_1)\sin(\varphi'+\psi)\sin(\varphi_1)}.$$

The proof of this Lemma is left as an exercise to the reader.

We can now combine these Lemmas in order to prove the thereom.

Figure 18 is a magnified view of the lower right corner of Figure 14 with extraneous information removed. We may now apply Lemmas 4.3, 4.4, and 4.5. Applying Lemma 4.3 we see

$$d(E_1,E_2) = \frac{d(p_8,I)\sin(\varphi_2+s)\sin(\varphi'-\varphi_1)\sin(s+\alpha+(\varphi_2-\varphi_1))}{\sin(\varphi'+s)\sin(\varphi_2-\varphi_1)\sin(s+\alpha+(\varphi'-\varphi_1))}.$$

Lemma 4.5 gives

$$d(D_2,\Sigma) = \frac{d(\Gamma,p_5)\sin(\varphi_2+\psi_2)\sin(\varphi_2+\psi')\sin(\varphi')}{\sin(\varphi'+\psi_2)\sin(\varphi'+\psi_2)\sin(\varphi_2)}.$$

Lemma 4.4 gives

$$d(D_1,D_2) = \frac{d(p_8,\Gamma)\sin(\varphi_2+\psi_1)\sin(\psi')\sin(\varphi_2+\psi'+B_1)\sin(\varphi_2-\varphi')}{\sin(\psi'-\psi_1)\sin(\varphi_2)\sin(\varphi'+\varphi')\sin((\varphi_2-\varphi')+B_1}.$$

For Σ' to exist, $d(E_1,E_2)$ must be smaller than $d(D_1,\Sigma)$. We will now solve $d(\Gamma,p_5)$ and $d(p_8,\Gamma)$ in terms of $d(\Gamma,p_2)$ in order to cancel distances. This Law of Sines calculation works out to

$$d(p_8,\Gamma) = \frac{d(\Gamma,p_2)\sin(\varphi_2+\psi_3)\sin(\psi'-\psi_1)}{\sin(\varphi_2+\psi_1)\sin(\psi_3-\psi')}$$

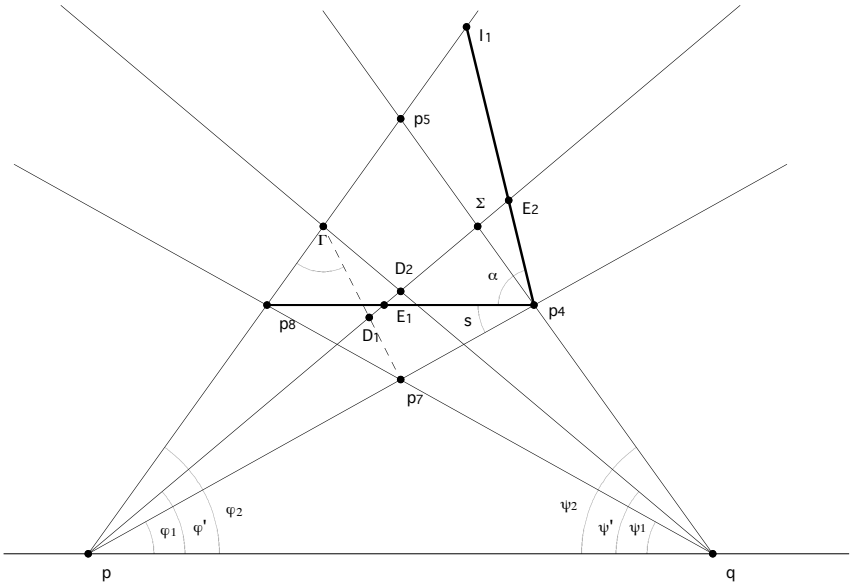

FIGURE 18. Magnified Section of Triangle Diagram

and

$$d(\Gamma, p_5) = \frac{d(\Gamma, p_2)\sin(\varphi_2 - \psi_3)\sin(\psi_2 - \psi')}{\sin(\varphi_2 + \psi_2)\sin(\psi_3 - \psi')}.$$

We now substitute this back into $d(D_1, \Sigma) = d(D_1, D_2) + (D_2, \Sigma)$ and factor

$$d(D_1, \Sigma) = \frac{d(\Gamma, p_2)\sin(\varphi_2 + \psi_3)}{\sin(\psi_3 - \psi')\sin(\varphi' + \varphi'\sin(\varphi_2)} \times$$

$$\left(\frac{\sin(\psi')\sin(\varphi_2 + \psi' + B_1)\sin(\varphi_2 - \varphi')}{\sin(\varphi_2 - \varphi' + B_1)} + \frac{\sin(\psi_2 - \psi')\sin(\varphi_2 + \psi')\sin(\varphi')}{\sin(\varphi' + \psi_2)} \right).$$

Since points Γ and Σ exist, we know the x-rays between the shadow body and the true triangle are equal. That is, with reference to both Figure 14 and Figure 18, $d(\Gamma, p_2) = d(p_8, I_1)$. Thus we may cancel distances on both sides of the inequality $d(E_1, E_2) < d(D_1, \Sigma)$.

Solutions for angles s, B_1 and $s + \alpha$ are derived by the usual method of solving for the tangent of angles and examining Figures 14 and 18. □

This theorem provides a method of determining when Γ' and Σ' will still show the shadow body might be convex. The main inequality is too complex to analyze numerically (and would not prove useful to the main aims of this paper), but graphical analysis via *Geometer's Sketchpad* shows that there are many such cases.

5. EXISTENCE RESULTS

Before beginning this project, the common assumption was that there existed no body sharing x-ray data with a polygon. Fithian [4] attempted to prove this for the triangle, but was unable to do

so in a final case. My own work began as an attempt to prove this final case, but soon signs pointed to the possibility that such a shadow body existed.

This section resulted from work done after assuming that the shadow body exists. Efforts were made to derive as much information as possible about the vertices of the shadow body. The lowest vertex at p_7 presented the easiest calculations, but the following theorems may be easily modified to deal with the other two vertices.

Steps taken to build points Γ and Σ and subsequent points directed our examination towards the likelihood of existence in situations of equality between corresponding angles φ_j and ψ_j (for $j = 1,2,3$). Several theorems derived previously in this paper have simpler analogs in this case.

In general, let the two x-ray sources be named, as before, *a* for the left source, and *b* for the right. Since we are dealing with a mirror image situation, it is only necessary to specify $\varphi_1, \varphi_2, \varphi_3$ and the distance from p to the point of reflection (this point is naturally halfway between *a* and *b* as *b* is the mirror image of *a*). We will call this reflection point *O* as it will be the origin of our coordinate system. Thus source *a* is located at $(-a,0)$ and source *b* at $(a,0)$.

A few other definitions will prove useful. The low vertex is the vertex of the shadow body located at the point that was previously called p_7. The side function is the function that defines the side of the shadow body connecting points p_7 and p_6. Due to symmetry, the side function from p_7 to p_6 will necessarily be a reflection of the side function from p_7 to p_2.

5.1. **Derivative Results.**

Theorem 5.1. *(Analog to Theorem 3.7) The interior angle, α, of the one tangent lines at a vertex is found by solving the following equation for α:*

$$\frac{d(a,O)\sin(2\alpha)}{\cos(\varphi)(\cos(2\alpha)+\cos(2\varphi))} - X_p'(\varphi) = 0.$$

2α corresponds to the sum of the interior angle reflected across the mirror; the tangent lines will necessarily be equal so a solution for 2α provides more than enough information.

Proof. The Law of Sines provides the entire proof. Looking at Figure 19, solve b_1 for $d(a,O)$:

$$b_1 = \frac{d(a,O)\sin(\pi/2)\sin(\varphi_1-\varphi)\sin(2\alpha)}{\sin(\pi/2+\varphi_1-\alpha)\sin(\pi/2-\varphi_1-\alpha)\sin(\pi/2-\varphi)}.$$

Divide by $\varphi_1 - \varphi$ and take the limit of both sides $\lim_{\varphi_1 \to \varphi}$. Simplification of the denominator is performed via the double angle identities. □

While proofs of a similar nature proved useful when attempting to show that the shadow body did not exist, they are only small steps along the way to proving that such a figure does exist. Thus we will investigate a method of determining convexity at the lower shadow vertex.

This method consists of examining the curvature operator at this location. In order to compute the operator, we need to find both first and second derivatives of the functions that make up the sides of the shadow body. As we are dealing only with the case where the angles of φ_j equal ψ_j, the functions making up the left and right side of the shadow body are equal as well. This will allow us to solve for the derivatives via a mathematically simple, albeit computationally complex method.

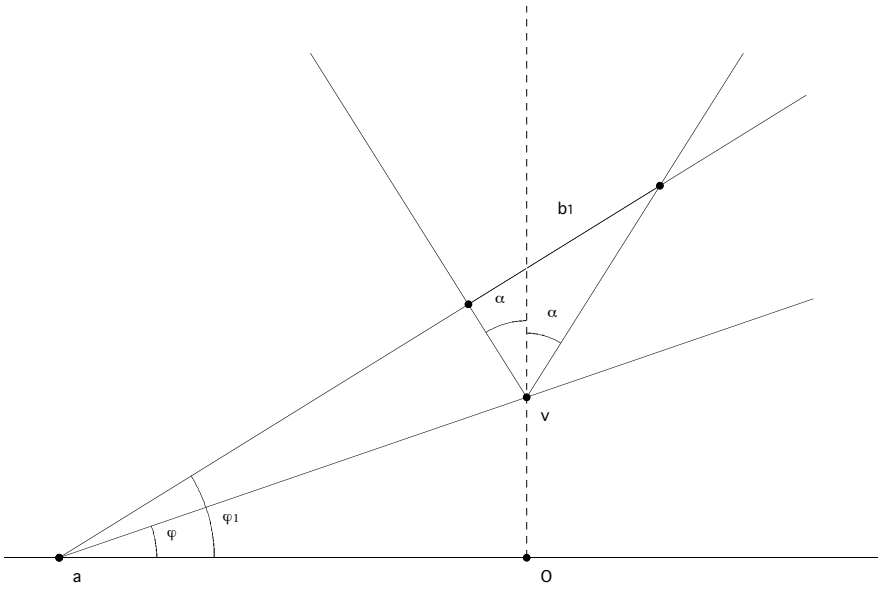

FIGURE 19. Illustration of Calculation of Tangent Lines in Reflection Case

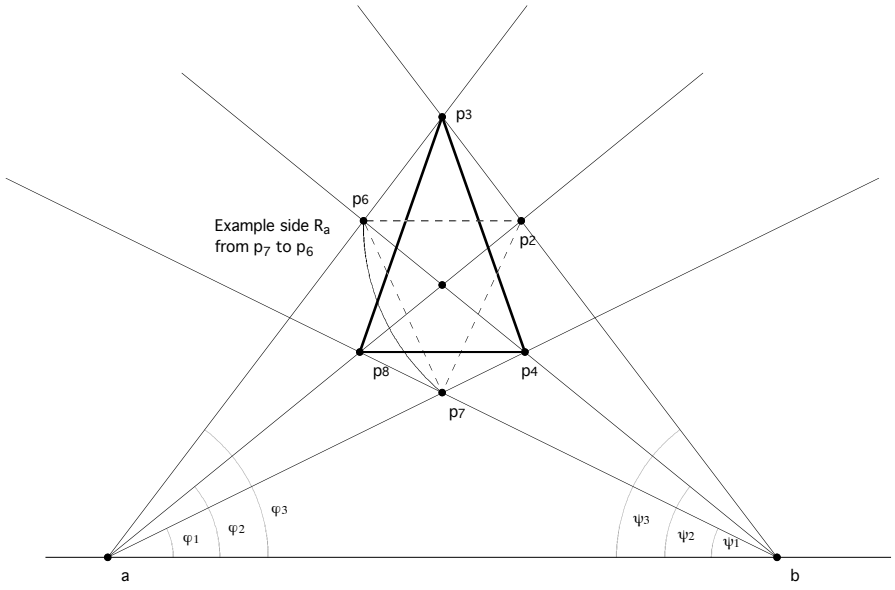

FIGURE 20. Illustration the Side Function between p_7 and p_6

Theorem 5.2. *The first derivative of the far side function R between p_7 and p_2, as seen in Figure 20 is*

$$R'_a(\varphi_1) = r_a(\varphi_1)\frac{r_a(\varphi_1)\sin(2\varphi_1) - r'_a(\varphi_1)\cos(2\varphi_1)}{r_a(\varphi_1)\cos(2\varphi_1) + r'_a(\varphi_1)\sin(2\varphi_1)}.$$

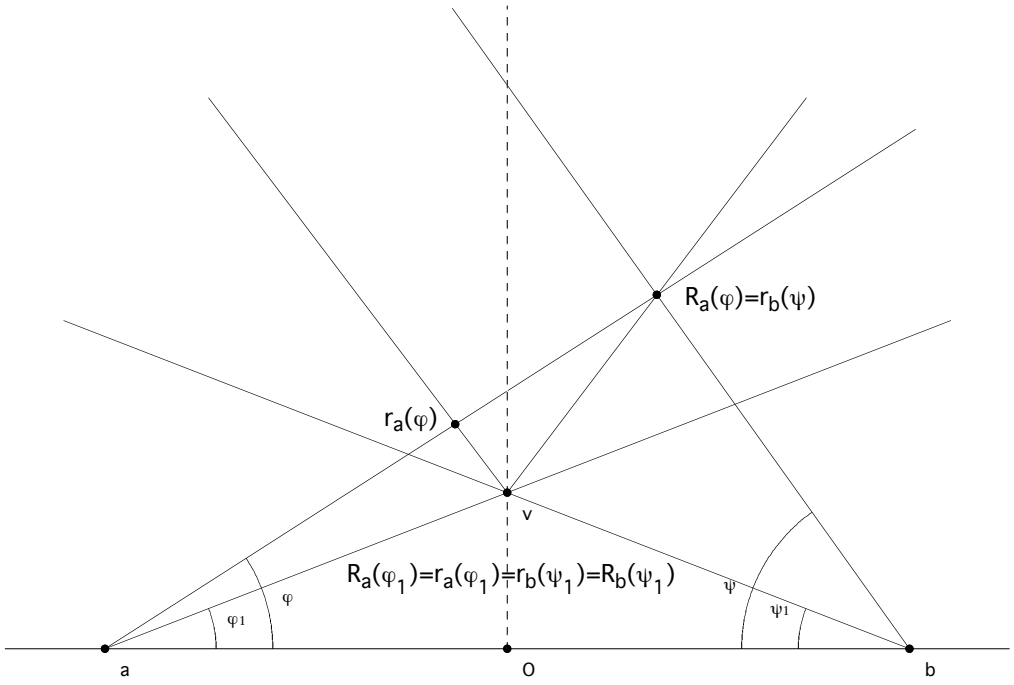

FIGURE 21. Illustration of First Derivative Calculation of Side Functions

Note. *In Figure 21, and subsequent such figures, the convex sides of the shadow body are represented as straight lines rather than the true convex curved lines which they are. This is used to simplify the diagrams and in no way represents the actual shadow body.*

Proof. Examining Figure 21, and applying both the Law of Sines and the Law of Cosines gives us two equations with which to begin:

$$R_a(\varphi)\sin(\varphi) = r_b(\psi)\sin(\psi)$$
$$(R_a(\varphi))^2 = (r_b(\psi))^2 + (b-a)^2 - 2(b-a)r_b(\psi)\cos(\psi).$$

Working with the former, we differentiate with respect to φ, remembering that ψ is a function of φ such that $\psi(\varphi_1) = \varphi_1$. This gives us

$$R_a(\varphi)\cos(\varphi) + R_a'(\varphi)\sin(\varphi) = (r_b(\psi)\cos(\psi) + r_b'(\psi)sin(\psi))\psi'(\varphi).$$

Solving for $\psi'(\varphi)$, which we shall use later produces

$$\psi'(\varphi) = \frac{R_a(\varphi)\cos(\varphi) + R_a'(\varphi)\sin(\varphi)}{r_b(\psi)\cos(\psi) + r_b'(\psi)sin(\psi)}.$$

This brings us to a Lemma that, while not currently used, may prove useful in the future.

Lemma 5.3. *We are now able to calculate $\psi'(\varphi_1)$. This is easily done by noting that, at φ_1, $R_a(\varphi_1) = r_b(\varphi_1)$, and $\cos(\varphi_1) = \frac{(b-a)/2}{r_b(\varphi_1)}$. Then*

$$\psi'(\varphi_1) = \frac{(b-a) + 2R_a'(\varphi_1)\sin(\varphi_1)}{(b-a) + 2r_b'(\varphi_1)\sin(\varphi_1)}.$$

We will now utilize the formula provided by the Law of Cosines. Differentiating both sides with respect to φ and simplifying gives us that

$$R_a(\varphi)R'_a(\varphi) = (r_b(\psi)r'_b(\psi) + (b-a)r_b(\psi)\sin(\psi) - (b-a)r'_b(\psi)\cos(\psi))\psi'(\varphi).$$

Substituting in our equation for $\psi'(\varphi)$, and evaluating the expression at φ_1 (although not utilizing Lemma 5.3) where $R_a = r_a = r_b = R_b$ and solving for $\frac{R'_a(\varphi_1)}{R_a(\varphi_1)}$ will provide us with the following equation. In an effort to simplify notation, I have removed the angle φ_1 from subsequent distances. Thus $R_a = r_a = r_a(\varphi_1) = d(a,v)$ where v is the low vertex.

$$\frac{R'_a}{R_a} = \frac{r_a r'_a \cos(\varphi_1) + (b-a)r_a \sin(\varphi_1)\cos(\varphi_1) - (b-a)r'_a \cos^2(\varphi_1)}{r_a^2 \cos(\varphi_1) - (b-a)r_a \sin^2(\varphi_1) + (b-a)r'_a \sin(\varphi_1)\cos(\varphi_1)}.$$

We will now simplify this equation to a more easily understood form. Applying the following identities to both numerator and denominator in the order they are related will modify the equation to the form shown in the statement of the theorem.

(1) From definition cosine: $r_a(\varphi_1)\cos(\varphi_1) = \frac{b-a}{2}$
(2) Sine Double Angle Identity: $2\sin(\varphi_1)\cos(\varphi_1) = \sin(2\varphi_1)$
(3) Cosine Double Angle Identity: $2\cos^2(\varphi_1) - 1 = 1 - 2\sin^2(\varphi_1) = \cos(2\varphi_1)$

□

As can be seen, this formula for $R'_a(\varphi_1)$ bears a close resemblance to the formula provided in Theorem 5.1. This is due to the relation between $X'_a(\varphi_1)$ and $R'_a(\varphi_1)$. Namely:

$$X'_a(\varphi_1) = R'_a(\varphi_1) - r'_a(\varphi_1).$$

This is a direct consequence of the definition of the x-ray as provided in Definition 2.4. More importantly, this allows us to solve the equation for $R'(\varphi_1)$ (or $r'(\varphi_1)$). Substituting this into Theorem 5.2 yields a quadratic equation to solve for $R'(\varphi_1)$

$$-R'^2\sin(2\varphi_1) + R'(X'\sin(2\varphi_1)) + X'r\cos(2\varphi_1) - r^2\sin(2\varphi_1) = 0$$

where all functions are evaluated at φ_1. This equation has two solutions, one positive and one negative, but we can dismiss one of them. A negative $R'(\varphi_1)$ means that the the far side point is moving further away as $\lim_{\varphi_1 \to \varphi}$. Since the vertex we are examining is located on the line of symmetry between our two sources, it is not possible that one side function of the shadow body crosses that line. We can thus dismiss this neagtive solution.

Graphically, this is shown in Figure 22. Circle C_1 is centered at source p and passes through p_2. A derivative of 0 points along the circle - here R is constant; the circle divides the picture into two regions: the region on the far side of the circle and the region on the near side. A negative derivative will point to the near side and cross the line of symmetry, a positive derivative will point to the far side thus be to the right side of the line of symmetry.

Remark. *If we take angle φ_1 to be $\pi/4$ then the equation for R' simplifies considerably*

$$-R'^2\sin(2(\pi/4)) + R'(X'\sin(2(\pi/4))) + X'r\cos(2(\pi/4)) - r^2\sin(2(\pi/4)) = -R'^2 + R'X' - r^2 = 0$$

This situation is not explored in this paper but points to a possible avenue for simplification of this, and future, derivative equations.

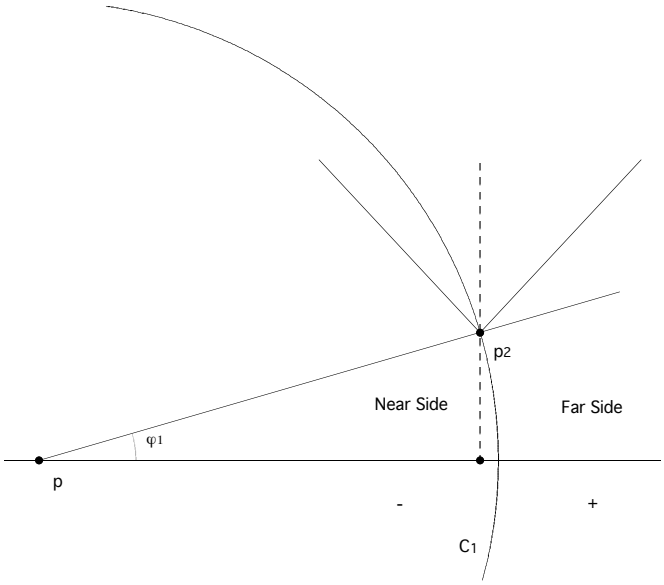

FIGURE 22. Illustration of Derivative Rejection

We know that the x-ray derivative of the shadow body at vertex p_7 from source p is equal to the x-ray derivative of the true triangle at vertex p_4 from source p. We can use Theorem 3.2 to calculate $X'(\varphi_1)$. This provides a numerical solution for $R'(\varphi_1)$.

Our analysis is now extended to the second derivative so that we may compute the curvature operator shown in Definition 2.7.

Theorem 5.4. *The second derivative of the far side function R between p_7 and p_2 is not displayed here. The solution is too long in length to include here and is, if needed, available via the simple Mathematica calculations described below.*

Proof. This is solved via the same method as Theorem 5.2. Take the second derivatives of the Law of Sines and Law of Cosines equations that were provided in Theorem 5.2 and solve for $\psi''(\varphi_1)$ in the former. Substitute it into the second derivative of the Law of Cosines equation and solve for $R''(\varphi_1)$. This process was carried out by Mathematica as the equations proved too long for by-hand computation. □

Remark. *Theorem 5.4 solves explicitly for $R''(\varphi_1)$ while Theorem 5.2 produces two results. This is to be expected from the derivation of $R''(\varphi_1)$. We do, in total, get two equations for $R''(\varphi_1)$ as we can plug each of our solutions for $R'(\varphi_1)$ into it. As mentioned before, we can dismiss one of these solutions and thus have just a single solution for $R''(\varphi_1)$.*

Using *Geometer's Sketchpad* the author discovered a triplet of angles $(\varphi_1, \varphi_2, \varphi_3)$, $(19.29^\circ, 32.32^\circ, 38.89^\circ)$ (with the ψ_js mirrored), that graphically showed the ability to map points up to Γ'''' and Σ'''' while retaining convexity of the resulting convex hull of shadow body boundary points.

We can use Theorem 5.2 to solve for $\psi'(\varphi_1)$ and $R'(\varphi_1)$. Corollary 3.5 provides a solution for $X''(\varphi_1)$, and Theorem 3.2 for $X'(\varphi_1)$ (as before). We can now compute the curvature operator for the numerical situation described above.

To begin, we need to find $X'_p(\varphi_1)$ and $X''_p(\varphi_1)$. These are obtained from the x-rays of the true triangle (due to x-ray equality). Both computations require the skew and skew + angle measurements for what is denoted ψ and ω in Figure 5. We have previously partially solved both of these angles. In Example 3.6 we solved for ψ^s which is the ψ we will use for our calculations. We also solved for what is called in Example 3.6 α. This is part of our ω. The other two parts are the ψ^s found above, and k_2 as calculated in Theorem 4.1. To summarize:

$$Our\ \psi = \psi^s \qquad (From\ Example\ 3.6)$$

$$Our\ \omega = \alpha + k_2 + \psi^s \qquad (From\ Example\ 3.6,\ Theorem\ 4.1,\ and Example\ 3.6,\ respectively).$$

Computing these shows $(\psi, \omega) = (93.18^\circ, 160.71^\circ)$

By the Law of Sines

$$d(p,v) = d(a,p_4) = d(a,p_7) + \frac{d(b,p_7)\sin(\psi_2 - \psi_1)}{\sin(\varphi_1 + \psi_2)}.$$

By our line of symmetry, $d(a,p_7) = d(b,p_7)$, thus

$$= d(a,p_7) + \frac{d(b,p_7)\sin(\psi_2 - \psi_1)}{\sin(\varphi_1 + \psi_2)} = \frac{d(a,O)\,(\sin(\varphi_1 + \psi_2) + \sin(\psi_2 - \psi_1))}{\sin(\varphi_1) + \psi_1}.$$

Regretfully, the author was unable to fully numerically analyze this situation due to time constraints.

6. Conclusion

The beginning of this paper was devoted to finding methods to show that no shadow body existed. When such methods failed, or became too complex to analyze, we analyzed the situation by assuming that the shadow body does exist in certain φ_j configurations. Graphical analysis showed the possibility that such solutions might exist, and enabled us to plot points up to Γ'''' and Σ''''. This strongly points to the existence of the shadow body in at least a few cases.

The curvature operator described by Black, Kimble, Koop, and Solmon [1] and Theorems 5.2 and 5.4 enable us to calculate the curvature, and hence the convexity of one side of the shadow body near the low vertex p_7. Assuming the curvature operator has the proper sign, this will indicate that there exists a neighborhood around the vertex with convexity; in fact, we know convexity for double the length of this interval as the situation will be mirrored on the other side. We can then use this known interval and the process we used to find points Γ' and Σ', Γ'' and Σ'', etc., to build sides of the shadow body. Whether the resulting shape will retain the convexity of this initial interval is unclear and a topic for future research.

References

[1] W. Black, J. Kimble, D. Koop, D.C. Solmon, Functions that are the Directed X-Ray of a Planar Convex Body. *To Appear In: Rend. Istit. Mat. Univ. Trieste*

[2] K.J. Falconer, X-ray Problems for Point Sources. *Proc. London Math. Soc.* (3) **46** (1983), 242-262.

[3] D. Fithian, Verifying a Triangle From Two Directed X-Rays. *Proc. REU-Oregon State U., 2002,* 242-262.

[4] D. Fithian, Verifying a Triangle With Two Directed X-Rays. *Undergraduate Thesis Oregon State U.* 2003
[5] R.J. Gardner, Symmetrals and X-rays of Planar Convex Bodies. *Arch. Math.* **41** (1983), 183-189.
[6] P.C. Hammer, Problem 2. In *Convexity*. Proceedings of Symposia in Pure Mathematics, vol. VII. American Mathematical Society, Providence, RI, 1963, pp. 498-499.
[7] D. Lam and D.C. Solmon, Reconstructing Convex Polygons in the Plane from One Drected X-ray. *Discrete and Comput. Geom.*, **26** (2001), 105-146.
[8] A. Volčič, A Three-Point Solution to Hammer's X-ray Problem. *J. London Math. Soc.* (2) **40** (1989), 171-178.

NORTHWESTERN UNIVERSITY
E-mail address: miller@set-theoretic.com